Determining the drivers and rates of soil erosion on the Loess Plateau since 1901

Pengfei Li[1], Jiannan Chen[1], Guangju Zhao[2,3*], Joseph Holden[4], Bintao Liu[5], Faith Ka Shun Chan[6], Jinfei Hu[1], Peili Wu[7], Xingmin Mu[2,8*]

[1]College of Geomatics, Xi'an University of Science and Technology, Xi'an 710054, China.

[2]State Key Laboratory of Soil Erosion and Dryland Farming on the Loess Plateau, Northwest A&F University, Yangling 712100, China.

[3]Institute of Soil and Water Conservation, Chinese Academy of Sciences & Ministry of Water Resources, Yangling 712100, China.

[4]water@leeds, School of Geography, University of Leeds, LS2 9JT, UK.

[5]Institute of Mountain Hazards and Environment, Chinese Academy of Sciences, Chengdu 610041, China.

[6]School of Geographical Science, University of Nottingham Ningbo China, Ningbo 315100, China.

[7]Met Office Hadley Centre, Exeter, UK.

[8]Huanghe research center of Hohai University, Hohai University, Nanjing 210098, China.

Corresponding author: Xingmin Mu（xmmu@ms.iswc.ac.cn）; Guangju Zhao (gjzhao@ms.iswc.ac.cn).

Highlights:

- We determined drivers and rates of erosion on the Loess Plateau (LP) since 1901.
- LP erosion rates increased during 1930s-1970s and declined during 1980s-2000s.
- Erosion rate changes before 2000s were primarily driven by land management.
- A recent increase in LP erosion rates was observed between 2010 and 2016.
- Erosion rate increase during 2010-2016 was mainly a result of extreme rainstorms.

Abstract

Attributing soil erosion to land management and climatic drivers is important for global policy development to protect soils. The Chinese Loess Plateau is one of the most eroded areas in the world. However, there has been limited assessment of historic spatial changes in erosion rates on the Loess Plateau and the major contributors driving these spatial changes. In this study, the Revised Universal Soil Loss Equation was empirically validated and employed to assess spatially distributed historical erosion rates on the Loess Plateau from 1901 to 2016. A double mass curve attribution technique was then used to investigate the impact of land management and climatic drivers on the Loess Plateau. Decadal average erosion rates and the total area with intensive erosion (> 5,000 t km^{-2} yr^{-1}) experienced a sharp increase from the 1930s to 1970s, followed by a decline to an historic low between the 1980s and 2000s. Mean erosion rates for the 2000s were 54.3% less than those of the 1970s. However, a recent increase in erosion rates was observed between 2010 and 2016. Land management change was the dominant driver of historical erosion rate changes before 2010. Extensive deforestation and farming, driven by population increase, were responsible for intensifying erosion between the 1930s and 1970s, while policy-driven conservation schemes and revegetation led to reduction thereafter. However, the recent increase in erosion between 2010 and 2016 was mainly driven by extreme rainfall events, a major concern given climate change projections. Advanced erosion control strategies are therefore required as part of integrated catchment management that both maintain water supplies for human use during dry periods while reducing erosion during storm events.

Keywords: Land degradation, spatiotemporal patterns, attribution analysis, modelling, conservation

1 Introduction

Soil erosion is a major global threat to terrestrial ecosystems (Borelli et al., 2017; 2020) with strong negative economic and environmental implications, including enhanced carbon loss (Armstrong, 2014; Li et al., 2017b; 2021a), reduced agricultural productivity (Montgomery, 2007), and aquatic pollution (Tong et al., 2017). It is thus crucial for achieving the Sustainable Development Goals, to understand the location and magnitude of erosion and the relationship with key impacting factors (Borrelli et al., 2020; Li et al., 2021c). Climate change and land management have been widely acknowledged as two major drivers of soil erosion, enhanced by the global scale of anthropogenic change since the start of the 20th century (Borrelli et al., 2020).

The Chinese Loess Plateau is one of the most eroded areas in the world (Wang et al., 2016; Li et al., 2017c; Best, 2019). Over 70% of the plateau is geomorphologically complex and characterized by deep gullies (thus steep slopes) (He et al., 2006). Soil erosion on the Loess Plateau was primarily a natural phenomenon before the middle Holocene, driven mainly by climate change as the geological environment is relatively stable (Liu et al., 2018). Since 3,000 years BP, human interventions increased (Ren and Zhu, 1994), including expansion of cultivation over the past 1,000 years driven by increasing population (Wu et al., 2020), deeply influencing erosion processes (Zhao et al., 2013). In particular, intensive human activities occurred during the 20th century, including those potentially accounting for erosion exacerbation (e.g. wars, agricultural production, deforestation) and large-scale soil conservation measures (e.g. ecological restoration, construction of dams and terraces) (He et al., 2006). These potential erosion acceleration and deceleration measures, along with climatic variations and changes (e.g. climate warming, extreme weather) may complicate the spatiotemporal pattern of soil erosion. To understand these spatio-temporal drivers first requires a reliable long-term historic erosion rate assessment.

River sediment load is often employed as a proxy for long-term erosion change (e.g. Borrelli et al., 2017; Sun et al., 2020; Wang et al., 2015; Zheng et al., 2019; Li et al., 2021a), as sediment yield data have often been collected at catchment outlets (Milliman and Farnsworth, 2016; Best et al., 2019; Wang and Sun, 2021). River sediment yield can be representative of soil erosion when hillslopes are well connected to catchment outlets (Evans et al., 2006; Zhao et al., 2013). However, huge check-dams and reservoirs established in river channels and gullies leads to a disconnection of soil erosion within catchments from sediment yield at catchment outlets (Evans and Warburton, 2005; Wang et al., 2021). Experimental manipulations, field observations, tracer studies, remote sensing monitoring and erosion modelling are also often employed to study erosion rates (Rodrigo-Comino, 2018). The former three are normally restricted to local-scale and short-term studies due to intensive labor and cost requirements. Remote sensing techniques can be used for a long-term and large-scale erosion study. However, remote sensing data are publicly accessible only from the 1980s onwards (Milodowski et al., 2020), limiting their application to a century-scale erosion study. Erosion models can be implemented over large regions for long periods (Borelli et al., 2017; Li et al., 2017b; 2017c), and if appropriately calibrated and validated, they provide a promising means for investigating historic erosion rates for the whole of the Loess Plateau.

Modelling efforts to assess water erosion rates are increasing, but most work has concentrated on sub-catchment and event scales (Li et al., 2017c). Erosion modelling for the entire Loess Plateau is still limited. To the authors' knowledge, there have been few studies assessing soil erosion rates across the Loess Plateau, and these focus on the 1980s onwards (Li et al., 2019; Sun et al., 2014). Erosion modelling for longer periods of the 20th century has never been undertaken for the entire plateau.

In this study, we assumed that the dominant driving factors of soil erosion rates varied during different periods. We validated the hypothesis through quantitatively assessing soil erosion by water since the start of 20th century (1901 to 2016) across the Loess Plateau, and determining the relative contribution of key drivers of changes in soil erosion rates over different periods. We used an empirical but physically plausible model, Revised Universal Soil Loss Equation (RUSLE) to model erosion rates and results were validated by historical sediment yield measurements. A double mass curve (DMC) technique was used to attribute the major contributors to changing erosion rates so that the role of land management and climatic drivers could be evaluated.

2 Materials and Methods

2.1 Study area

The Loess Plateau (33°41´ N–41°16´ N, 100°52´ E–114°33´ E) spans horizontally over 640,000 km^2 and vertically between 1000 m and 1600 m above sea level (Zhao et al., 2013), including six regions: the hilly and gully plateau (140,000 km^2), the high-plain plateau (200,000 km^2), deserts (79,200 km^2), the rocky mountainous area (107,200 km^2), the Fen-Wei river valley (63,600 km^2) and the Hetao alluvial plains (58,700 km^2) (Figure S1). The plateau is characterized by deep gullies and steep slopes developed on thick loess deposits, accumulated by wind deposits from the Gobi desert during the Quaternary (Cai, 2001). The loess is loose, porous and easily detached by erosive forces (Li et al., 2021b), including raindrop action, running water, gravity, freeze-thaw and wind (Li et al., 2017c). The plateau is located in the arid and semiarid climate zone (Yang et al., 2018), with mean annual precipitation ranging from 150 mm in the northwest to 700 mm in the southeast (Zhao et al., 2013). Precipitation is much lower than potential evapotranspiration (Tsunekawa et al., 2014), leading to a low soil water content and thus limited growth of vegetation (Jiao et al., 2016). The precipitation mainly takes place in summer months (July to September) in the form of intensive and short-duration rainfall events (Guan et al., 2021), which act as a major erosive agent on the Loess Plateau. Human activities (e.g. agricultural production, wars, deforestation, revegetation, conservation measures) are also thought to have impacted the initiation and development of erosion, particularly since the start of the 20^{th} century (He et al., 2006).

2.2 Assessment of spatially distributed erosion rates

2.2.1 RUSLE description and implementation

RUSLE (Equation 1) was developed for estimating soil loss driven by rill and inter-rill erosion based on measurements in the United States (Renard et al., 1991). The model has been adapted for the erosion condition on the Loess Plateau, mainly through taking account of steep slope erosion processes (Liu et al., 1994). Although being spatially lumped, RUSLE can be used to assess soil erosion rates over large areas as a spatially distributed model, through dividing the study area into small sub-units with uniform characteristics (i.e. grid cells).

$$A = R * K * LS * C * P \quad (1)$$

where *A* is the estimated soil loss per unit area per unit time (t ha^{-1} yr^{-1}); *R* is the rainfall-runoff erosivity factor (MJ mm ha^{-1} h^{-1} yr^{-1}), and represents the driving force of erosion; *K* is the soil erodibility factor (t ha h ha^{-1} MJ^{-1} mm^{-1}), reflecting the susceptibility of soil to erosion; *LS* is the slope length and slope gradient factors, reflecting the effect of slope length and slope gradient on erosion; *C* is the vegetation cover factor, accounting for the impact of vegetation coverage on soil erosion; and *P* is the erosion control practice factor, representing the benefit of a given conservation measure for soil loss.

In the study, RUSLE was operated at a 1-km resolution, with reference to that of the available datasets. The *R* factor was traditionally derived based on rainfall energy (E) and 30-min rainfall intensity (I30). However, E and I30 are often unavailable. On the Loess Plateau the algorithms developed by Zhang and Fu (2003) have been widely accepted and applied to derive rainfall erosivity based on more accessible daily, monthly and annual precipitation measurements. In our study, the annual rainfall erosivity (Figure S2) was assessed using algorithms based on 1-km monthly precipitation grid data for 1901-2016 derived from the CHELSAcruts dataset (https://chelsa-climate.org/chelsacruts/) (Equations 2 and 3) (Karger and Zimmermann, 2018):

$$R = 0.3589F^{1.9462} \quad (2)$$

$$F = [\sum_{i=1}^{12} P_i^2] \times P^{-1} \quad (3)$$

where P is annual precipitation, mm; P_i is the precipitation for the ith month, mm; R is annual rainfall erosivity (MJ mm ha^{-1} h^{-1} yr^{-1}), and F is the dimensionless factor accounting for the seasonal variations in precipitation.

The K factor was calculated by the method (Equation 4) employed in the EPIC model, which has been widely applied on the Loess Plateau due to a low data requirement (e.g. Li et al., 2020b; Sun et al., 2014), based on soil type and properties provided by Soil Science Database of China (http://vdb3.soil.csdb.cn/extend/jsp/introduction). The estimated K factor was further improved by Equation 5 to eliminate its deviation from a field measured K factor (Figure S2) (Zhang et al., 2007).

$$K_{EPIC} = 0.1317 \left\{0.2 + 0.3\, exp\left[-0.0256San\left(1 - \frac{Sil}{100}\right)\right]\right\} * \left(\frac{Sil}{Cla+Sil}\right)^{0.3}\left(1 - \frac{0.25C}{C+exp(3.72-2.95C)}\right)^{*}\left(1 - \frac{0.75Sn}{Sn+exp(-5.51+22.95Sn)}\right) \quad (4)$$

$$K = -0.01383 + 0.51575\, K_{EPIC} \quad (5)$$

where San, Sil and Cla are the sand fraction (%), silt fraction (%), and clay fraction (%), respectively; C represents soil organic carbon content (%); Sn equals 1-San/100, K_{EPIC} is the erodibility estimated by the EPIC model, and 0.1317 is a dimensionless conversion factor that converts the unit of estimated erodibility from the American system to the international standard system.

The *LS* factor was derived based on the 1-km DEM, which was resampled from the 30-m DEM provided by the Advanced Spaceborne Thermal Emission and Reflection radiometer Global Digital Elevation Model version 2 (ASTER GDEM V2) (https://nordpil.com/blog/aster-gdem/). Traditional *LS* calculation algorithms are suitable for ≤ 18% slopes rather than > 18% slopes that are widespread on the Loess Plateau (McCool et al., 1989), while soil loss from 9% to 55% slopes is linearly related to the sine of the slope gradient (Liu et al., 1994). Thus, traditional S factor derivation formulae developed by McCool et al. (1989; 1997) were used for ≤ 18% area, and the formula developed by Liu et al. (1994) was employed for > 18% slopes (Figure S2) (Equation 6). The *L* factor was derived using the method which was developed by Jiang et al. (2005) through synthesizing field measurements mainly from the Loess Plateau (Equation 7).

$$S = \begin{cases} 10.8\, sin\,\theta + 0.03, & 9\% > \theta > 0 \\ 16.8 \sin\theta - 0.5, & 18\% \geq \theta \geq 9\% \\ 21.91 \sin\theta - 0.96, & \theta > 18\% \end{cases} \quad (6)$$

$$L = \left(\frac{\Upsilon}{20}\right)^m \quad \begin{cases} m = 0.45 & \theta \geq 40\% \\ m = 0.35 & 40\% > \theta \geq 21\% \\ m = 0.2 & 21\% > \theta \geq 9\% \\ m = 0.15 & 9\% > \theta \geq 0 \end{cases} \quad (7)$$

where, Υ is the slope length (m), and *m* is a dimensionless constant depending on the percent slope (θ).

The C factor was derived separately for different land-use types on the Loess Plateau, which were defined as artificial land (e.g. urban area, villages, built-up area), croplands, forest and grassland, and water body with reference to the 1-km resolution land-se data resampled from the History Database of the Global Environment version 3.2.1 (HYDE 3.2.1) (Klein Goldewijk et al., 2017). The HYDE 3.2.1 dataset provides 5-minute (~8 km) resolution land-use maps for the past 12,000 years. It is an update and extension of the HYDE dataset, which is an internally consistent combination of historical population estimates and allocation algorithms with time-dependent weighting maps for land use (Klein Goldewijk et al., 2017). The C factor for forest and grassland was calculated by Equation 8, while that for croplands was estimated by Equation 9 (Figure S2). They were developed based on a regression analysis between the field measured C factor for corresponding sampling units of the national soil erosion survey of China completed in 2011 (Liu et al., 2020) and 1-km NDVI derived from Moderate-Resolution Imaging Spectroradiometer (MODIS) data. The C factor for water bodies and artificial land was set to 0.001 and 0.1, which accounts for the soil conservation function.

$$C = 1.2899 \times e^{-6.343 \times NDVI} \quad R^2 = 0.7531 \quad p < 0.05 \tag{8}$$

$$C = -0.143 \times ln(NDVI) + 0.2525 \quad R^2 = 0.539 \quad p < 0.05 \tag{9}$$

The NDVI data, derived from satellite images, were only available after 1982, making the calculation of the C factor for the whole study period difficult. Given that precipitation is a major water source for vegetation on the Loess Plateau (Li et al., 2017a; Xin et al., 2008), the spatial distribution of vegetation is closely related to patterns of precipitation and relative humidity (Kong et al., 2018). Therefore it should be possible to predict vegetation cover using precipitation data. In line with this, a linear relationship ($R^2 = 0.77$, $p < 0.001$) was established between monthly precipitation and NDVI during 2000-2016 derived from the MODIS dataset. In order to ensure the consistency of the NDVI throughout the time, the regression equation was then applied to reconstruct the NDVI for the whole of the study period based on the monthly precipitation derived from the CHELSAcruts dataset.

The *P* factor was derived based on the resampled HYDE 3.2.1 data (1 km resolution) and the 300-m resolution Climate Change Initiative Land Cover (CCI_LC) dataset (https://www.esa-landcover-cci.org/?q=node/164), through incorporating terraces as the dominating control factor. The CCI-LC maps were produced using multiple algorithms required for the generation of global land cover products that are stable and consistent over time, mainly based on the Envisat MERIS archive and SPOT-Vegetation time series (Bontemps et al., 2015). The cropland of the Loess Plateau (as defined for the C factor derivation) was further divided into terraces and sloping croplands in terms of the DEM and CCI_LC dataset, which offers a detailed distribution of rain-fed and irrigated croplands (Bontemps et al., 2015). Terraces were considered as the irrigated croplands and gently-sloping rain-fed croplands (slope of < 3°). The *P* factor value of terraces and artificial land was set to 0.2 and 0.01 respectively with reference to previous studies (e.g. Sun et al., 2014), while that of forest and grassland, water body and sloping cropland was set to 1 through assuming that there was no erosion control practice (Figure S2). The CCI_LC data were only available from 1992 onwards. Therefore, the spatial distribution of terraces before 1992 was considered the same as that of 1992. This is a compromise considering data shortage but acceptable because the majority of the terraces on the Loess Plateau were constructed from the 1990s onwards (Mu et al., 2019).

2.2.2 Model validation

Validation of large-scale modelling results remains a challenge (Batista et al., 2019; Wen and Deng, 2020). RUSLE predicts soil loss driven by rills and interrills and theoretically should be validated by erosion rate measurements, which were rather limited for the Loess Plateau (Li et al., 2020b). The model was operated at a spatial resolution of 1 km, which is much greater than the plots used for erosion rate monitoring. Therefore, it was difficult to validate our modelling results with measured erosion rates.

Measured sediment yield from catchments provides an alternative for validation. The sediment delivery ratio on the plateau was close to 1 before large-scale construction of check dams (i.e. 1970) (Zhao et al., 2013). Therefore, sediment yields from 22 catchments (Figure S1) between 1919 and 1969 (six catchments for 1919-1953 and 16 catchments for 1957-1969) obtained from the Yellow River Conservancy Commission were employed to validate RUSLE predictions. Sediment yield measurements from the initial six catchments were jointly used for model validation as the measurements were limited before 1950.

2.2.3 Assessment of spatiotemporal patterns of erosion rates

Temporal patterns of modelled erosion rates during 1901-2016 were investigated based on annual time series and the decadal average of erosion rates for the entire Loess Plateau and its six subregions. Spatial patterns of erosion rates during 1901-2016 and extreme erosion years (erosion rate > 10,000 t km-2 yr-1) were assessed through categorizing erosion rates into different levels. These levels were defined by the technological standard of soil and water conservation (SL190-2007) issued by the Ministry of Water Resources of China (MWRC) (Sun et al., 2014). The MWRC-defined erosion intensity levels consist of weak erosion (< 1,000 t km-2 yr-1), slight erosion (1,000-2,500 t km-2 yr-1), moderate erosion (2,500-5,000 t km-2 yr-1), intensive erosion (5,000-8,000 t km-2 yr-1), very intensive erosion (8,000-15,000 t km-2 yr-1) and severe erosion (> 15,000 t km-2 yr-1). The proportion of each area containing erosion rates at each intensity level was calculated and all spatial analysis in the study was completed using the ArcGIS 10.2 package.

2.3 Separation of impacts of precipitation and human activities

A double mass curve (DMC) approach (Searcy and Hardison, 1960) was employed to quantitatively evaluate the impact of climate change (i.e. precipitation) and human activities on soil erosion. The DMC is advantageous for its low data requirement and high transferability. The DMC is composed of cumulative values of two parameters plotted against one another (i.e. x and y coordinates) through a specific period. The DMC is a straight line when the ratio of x and y is a constant, while change points (slope breaks) in the DMC are interpreted as a result of external disturbances. The deviation of DMC from the straight line represents the contribution of external disturbances. In the study, the DMC was established based on cumulative values of precipitation (x axis) and erosion rates (y axis) (Figure S3). The deviation of DMC from the straight line was used to quantitatively evaluate the contribution of precipitation ($\Delta_{\text{Precipitation}}$ in Figure S3) and human activities ($\Delta_{\text{Human activity}}$ in Figure S3) on soil erosion.

The change point of the DMC is essential for the separation of the contribution of precipitation and human activities in different periods. In the study, the change point was determined visually, with the aid of the trend analysis for modelled erosion rates. The cumulative sums (CUSUM) of the differences between monthly means and the grand mean of each data set function, proposed by Cluis (1983), was employed to conduct the trend analysis. The function has been applied to study the changing trend (thus changing points) of sediment discharge over the Loess Plateau (Mu et al., 2012), and it can be derived using Equation 10:

$$LP_i = \sum_1^n (E_i - \bar{E}) \quad (10)$$

where, LP_i is the CUSUM for the i^{th} year, E_i is erosion rates for the i^{th} year, $\bar{E}$ is mean annual erosion rates for the study period, and n is the number of years (116 years).

2.4 Statistical analysis

In the study, the unitary linear regression method was employed to fit the relation between variables (Equations 11-13):

$$y = ax + b \quad (11)$$

$$a = \frac{n\sum x_i y_i - \sum x_i \sum y_i}{n\sum x_i^2 - (\sum x_i)^2} \quad (12)$$

$$b = \frac{\sum y_i}{n} - a\frac{\sum x_i}{n} \quad (13)$$

where a and b represent the parameters of the linear regression equation, x and y represent the independent and dependent variable respectively, and i refers to the values of x and y in i^{th} period. The goodness of the fit was assessed using the coefficient of determination

(R^2) (Equation 14), while the significance of the regression was evaluated using the F test (i.e. p value).

$$R^2 = \left[\frac{\sum(o_i - \bar{o})(p_i - \bar{p})}{\sqrt{\sum(o_i - \bar{o})^2}\sqrt{\sum(p_i - \bar{p})^2}}\right]^2 \quad (14)$$

where o_i and p_i represent the observed and predicted values in the i period, and $\bar{o}$ and $\bar{p}$ refer to the average of o_i and p_i. Statistical analysis was performed in Microsoft Excel 2013.

3 Results

3.1 Accuracy of modelling results

The R^2 between modelling results and sediment yield for 1919-1953 was 0.75, while that for 1957-1969 was over 0.48 (Table 1). The fitness of modelling results and observations was not perfect, but satisfactory, given that data availability and data quality of the RUSLE input parameters were limited (e.g. measured NDVI was not available for the validation period).

Table 1. Validation of RUSLE modelling results with sediment yield measured at catchment outlets

Period	Stations	Drainage area (km^2)	R^2	*p*
1957-1969	Huangfuchuan	3175	0.74	< 0.001**
	Qingshui	735	0.77	<0.001**
	Jiuxian	1562	0.55	0.004*
	Pianguan	1915	0.58	0.002*
	Gaoshiya	1263	0.69	< 0.001**
	Qiaotou	2901	0.80	< 0.001**
	Peijiachuan	2159	0.71	< 0.001**
	Xingxian	650	0.51	0.006*
	Shenjiawan	1121	0.63	0.001*
	Gaojiachuan	3253	0.74	< 0.001**
	Linjiaping	1873	0.70	< 0.001**
	Houdacheng	4102	0.72	< 0.001**
	Yanchuan	3468	0.48	0.008*
	Daning	3992	0.73	< 0.001**
	Baijiachuan	29662	0.59	0.002*
	Jixian	436	0.59	0.002*
1919-1953	Xiangtang	15750	0.75	< 0.001**
	Jingle	3100		
	Lancun	7600		
	Zhaocheng	27700		
	Zhuangtou	26700		
	Nanhechuan	26550		

* significant at p < 0.01, ** significant at p < 0.001

3.2 Spatiotemporal changes of erosion rates

Modelled erosion rates varied greatly during 1901-2016 (Figure S1). The overall erosion rates, as well as for the six subregions, were generally low until 1917, where we see a peak of 27,940.3 t km^{-2} yr^{-1} for the hilly and gully plateau. The mean overall erosion rate for the 1920s increased to 5,663.0 t km^{-2} yr^{-1} compared to 4,928.7 t km^{-2} yr^{-1} for the 1910s, partly due to an extreme event in 1925. The amplitude of changes in erosion rates was variable across the subregions, with intensified erosion in the high-plain plateau and Hetao alluvial plains while there was reduced erosion in the other four regions. During the 1930s to 1970s, erosion rates stayed at a relatively high level and mean erosion rates exceeded 8,000 t km^{-2} yr^{-1} for 13 years during that period. During the 1980s to 2000s, erosion rates decreased markedly. Erosion rates on the Loess Plateau and its six subregions for the 2000s were 54.3% and 51.1%-66.2% lower than that for the 1970s and were even smaller than that for the 1900s and 1910s. However, during 2010 to 2016, the erosion rates rebounded to a level comparable with that of 1900s and 1910s. This increase was largely attributed to particularly intensive erosion in 2013 (10,960.8 km^{-2} yr^{-1}).

Erosion rates also varied greatly among regions (Figure 1). Mean erosion rates during 1901-2016 for the subregions followed the sequence of hilly and gully plateau > high-plain plateau > rocky mountainous area > Fen-Wei river valley > Hetao alluvial plains > deserts. Very intensive erosion (> 8,000 t km^{-2} yr^{-1}) was mainly concentrated in the hilly and gully plateau and high-plain plateau. In the early 20th century (1900s and 1910s), the very intensive erosion was mainly restricted to the hilly and gully plateau. Since the 1920s very intensive erosion began to extend to the high-plain plateau and the rocky mountainous area. Since the 1980s soil erosion reduced and the areas of very intensive erosion retreated to the northeastern part of the high-plain plateau and southern part of the hilly and gully plateau (i.e. central Loess Plateau). However, the area of very intensive erosion increased again during 2010-2016.

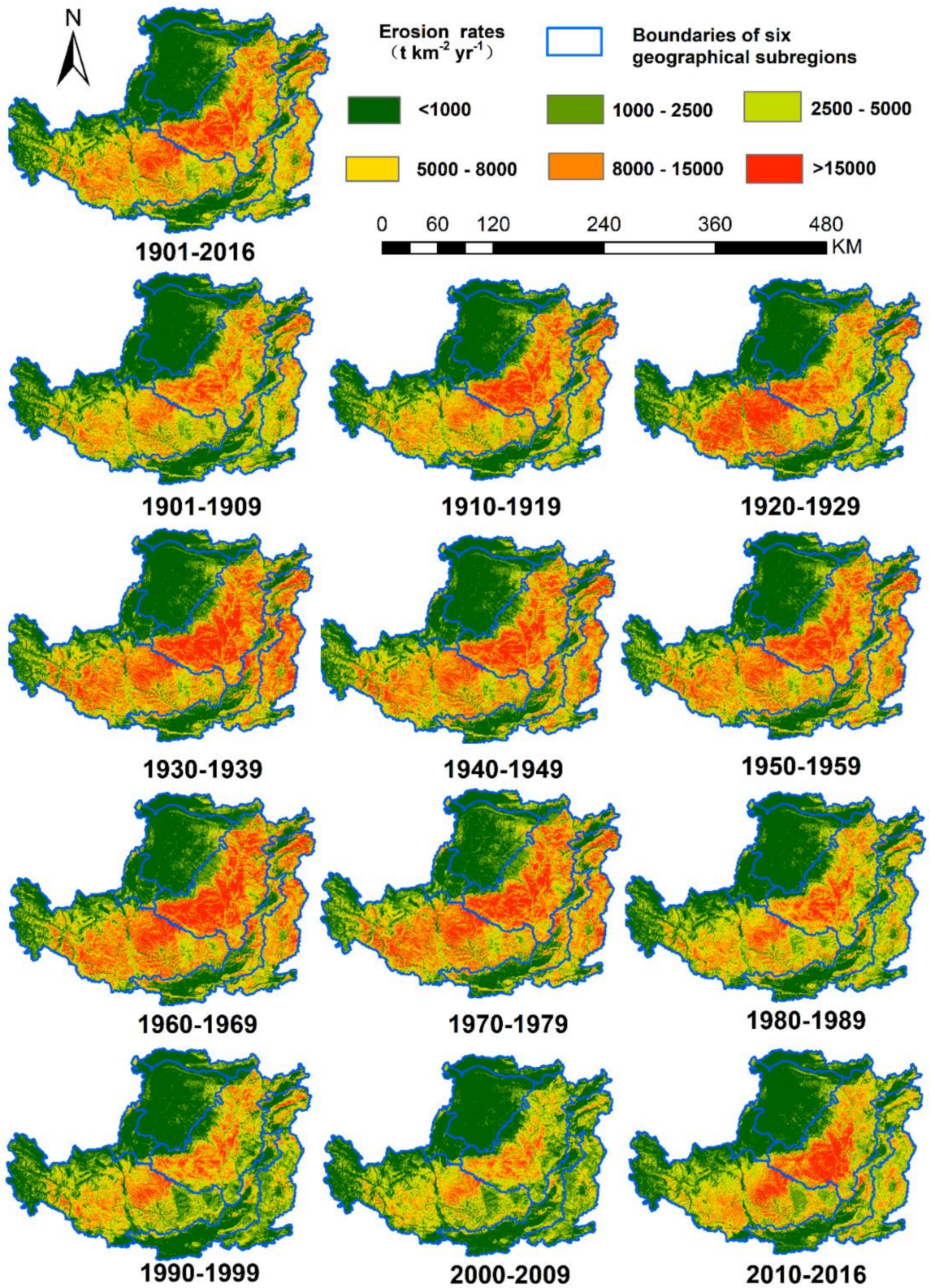

Figure 1. Spatiotemporal patterns of soil erosion rates over the Loess Plateau and 10-year average erosion rates for the Loess Plateau between 1901 and 2016.

An erosion rate of < 5,000 t km^{-2} yr^{-1} accounted for 54.6%-81.3% of the area of the Loess Plateau, particularly before 1930 and after 1980 (Figure 2). This is partly because 67.8%-99.7% of the Fen-Wei river valley, deserts and Hetao alluvial plains were subject to erosion with a rate < 5,000 t km^{-2} yr^{-1}. Erosion rates of > 5,000 t km^{-2} yr^{-1} occupied 56.2%- 72.2% of the hilly and gully plateau before the 1970s and 36.2%-56.0% of the region since the 1980s. In the high-plain plateau, the total area with erosion rates > 5,000 t km^{-2} yr^{-1} (50.2 %- 53.4% of the region) was of similar magnitude to that of the total area with an erosion rate < 5,000 t km^{-2} yr^{-1} (46.6%-49.8% of the region) between the 1920s and 1970s. Erosion rates < 5,000 t km^{-2} yr^{-1} accounted for 59.2%- 75.6% of the high-plain plateau during other periods. In the rocky mountainous area, the total area with erosion rates > 5,000 t km^{-2} yr^{-1} (40.8%-52.4% of the region) was similar to the total area with erosion rates < 5,000 t km^{-2} yr^{-1} (47.6%-59.2% of the area) before the 1920s. The former accounted for 57.8%-67.1% of the area between the 1930s and 1970s, while the latter occupied 69.6%-87.4% of the area since the 1980s. Notably, intensive erosion (> 5,000 t km^{-2} yr^{-1}) expanded during 2010-2016 in all six subregions.

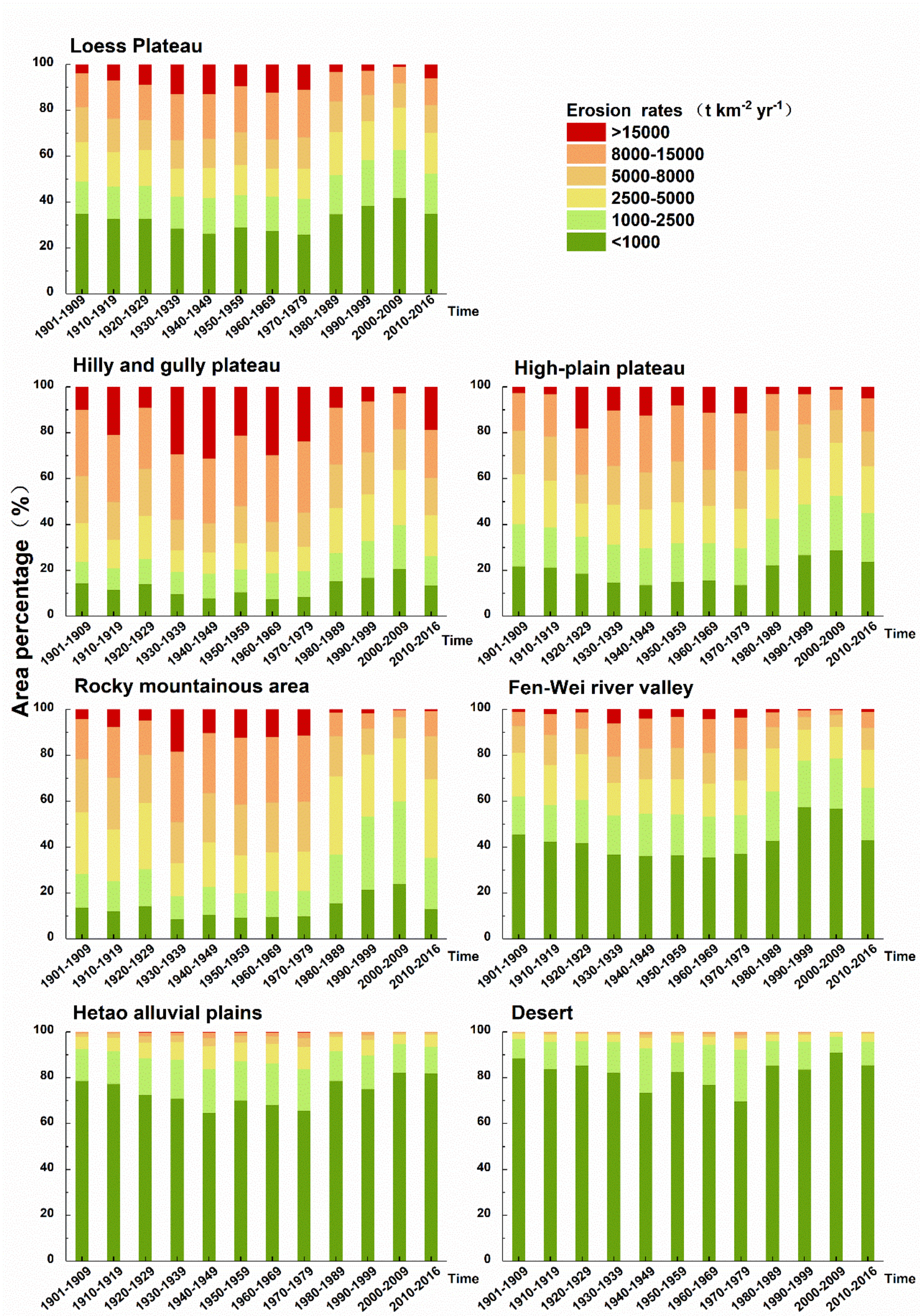

Figure 2. Temporal variations in area percentage of different levels of erosion for the Loess Plateau and the six geographical subregions of the Loess Plateau between 1901 and 2016.

Between 1901 and 2016, mean erosion rates of the Loess Plateau exceeded 10,000 t km^{-2} yr^{-1} in four years, which were 1917, 1925, 1949 and 2013. In these four years, very intensive erosion (> 8,000 km^{-2} yr^{-1}) was concentrated in the hilly and gully plateau and high-plain plateau (Figure 3). In 2013, the very intensively eroded area (> 8,000 km^{-2} yr^{-1}) was less than that in 1917, 1925 and 1949, except for in the high-plain plateau where the total area with the highest intensity erosion was greater compared to 1917 (Figure 4). Extreme erosion rates corresponded well with intensive rainfall in rainy months (i.e. June to September). For example, in 2013, the high erosion rates were coincident with peak precipitation in July, which is particularly the case for the hilly and gully plateau (Figure 5).

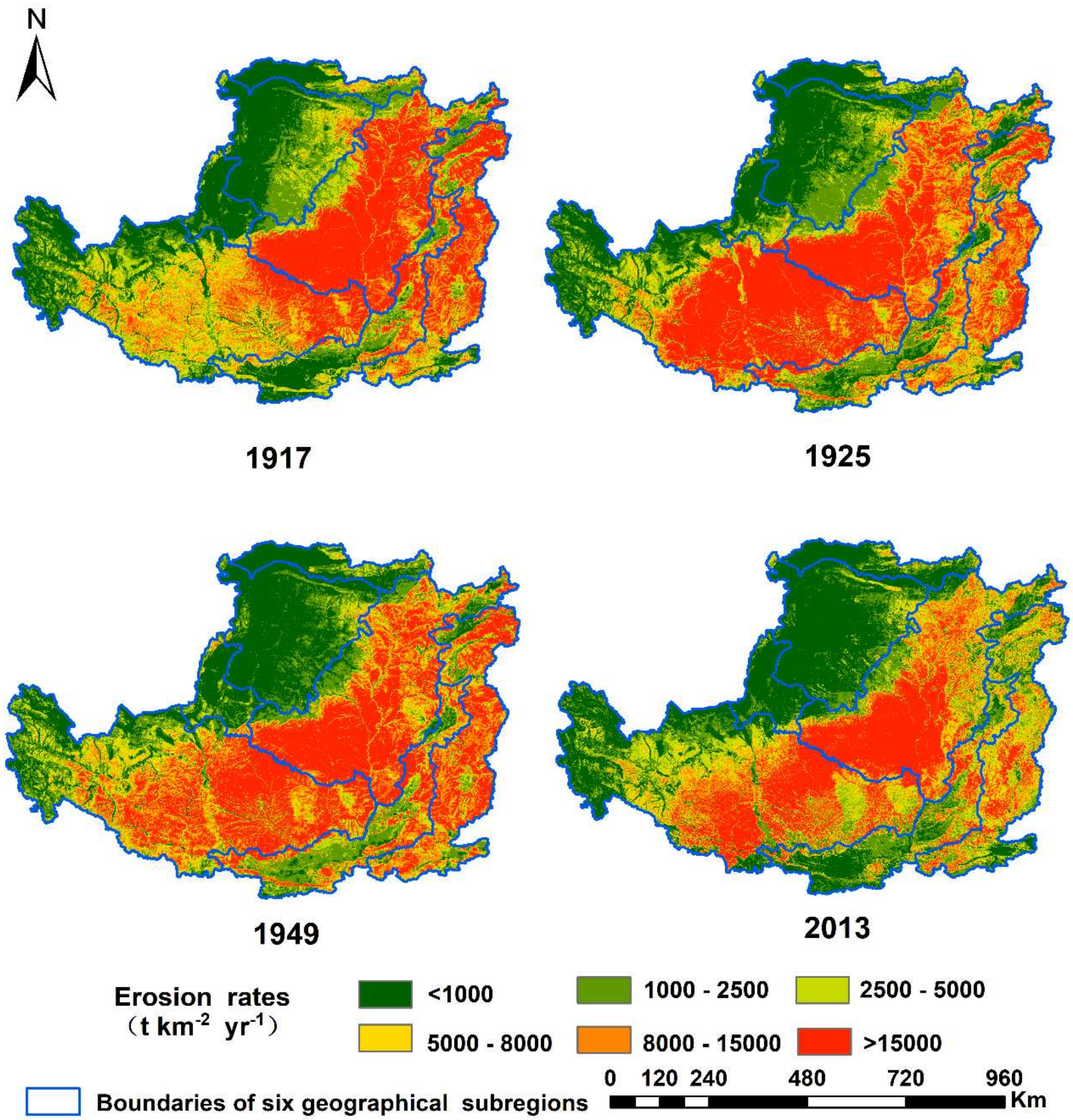

Figure 3. Spatial patterns of soil erosion rates over the Loess Plateau for extreme erosion years, during which mean soil erosion rates for the Loess Plateau were >10,000 t km^{-2} yr^{-1}.

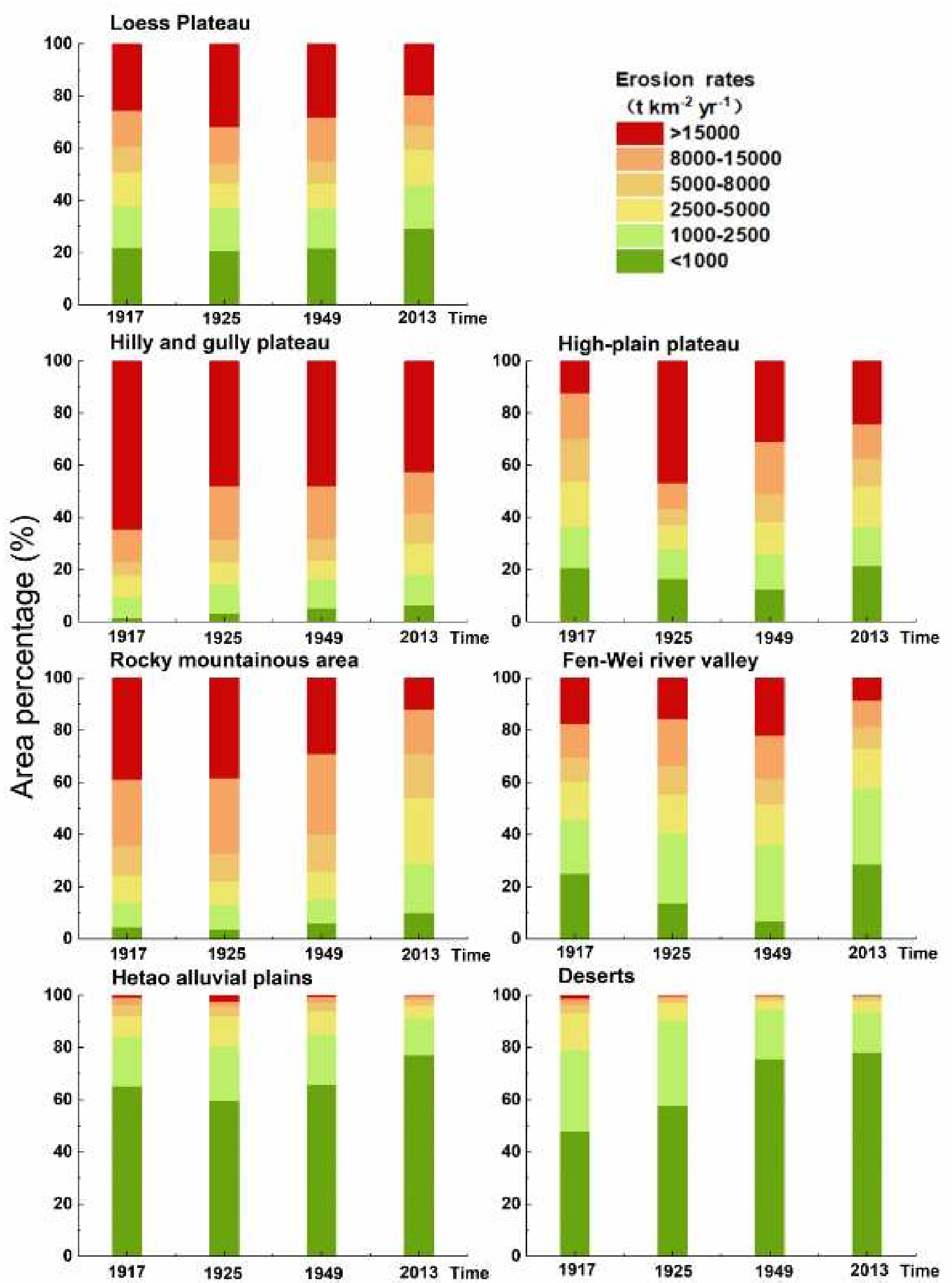

Figure 4. Area percentage of different levels of erosion for the Loess Plateau and six geographical subregions during extreme erosion years (i.e. 1917, 1925, 1949 and 2013).

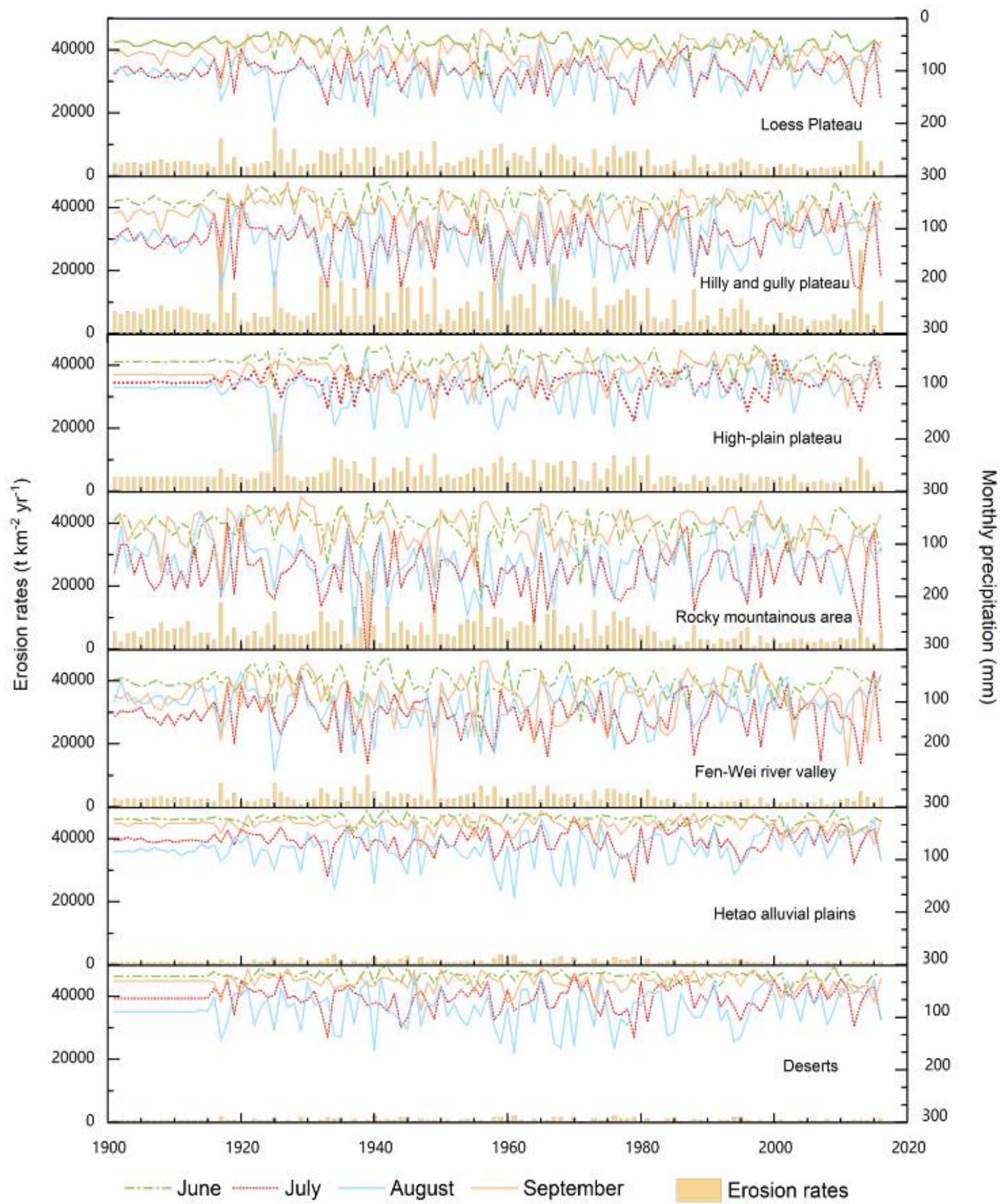

Figure 5. Time series of RUSLE predicted annual erosion rates and monthly precipitation for rainy months (i.e. June, July, August and September).

3.3 Impacts of natural and human factors on erosion rates

In terms of the DMC and CUSUM analysis, two change points were found for the modelled erosion rates. They are 1924 and 1981 for the entire Loess Plateau, high-plain plateau and Hetao alluvial plains, and 1931 and 1981 for the hilly and gully plateau, rocky mountainous area, Fen-Wei river valley, and deserts (Figure S3 and Figure S4). The CUSUM of soil erosion rates followed a decreasing trend during 1901-1924/1931 and 1981-2016, and an increasing trend during 1925/1931-1980 for corresponding areas.

DMC analysis showed that, compared to the reference period, erosion rates increased during 1925/1932-1981 and decreased after 1982 (Table 2). In addition, the erosion increases during 1925/1932-1981 were dominated by human interventions (the contribution of human activities was over 53%), particularly for the high-plain plateau and Hetao alluvial plains (the contribution of human activities was over 96%). The decrease of erosion between 1982 and 2016 was also dominated by human interventions, of which the contribution was no less than 68%. The contribution of human interventions to erosion decrease often exceeded 100% as precipitation facilitated an erosion increase. Precipitation changes intensify erosion on the Loess Plateau and most of its subregions (except High-plain plateau and Hetao alluvial plains), but the contribution of precipitation change to erosion rate changes were much lower than that of human activities.

Table 2 The impact of precipitation and human interventions on changes in erosion rates for the Loess Plateau

Region	Period	observed mean ($t\ km^{-2}\ yr^{-1}$)	modelled mean ($t\ km^{-2}\ yr^{-1}$)	Total change[a]		Precipitation contribution[b]		Human contribution[c]	
				Amount ($t\ km^{-2}\ yr^{-1}$)	Percent (%)	Amount ($t\ km^{-2}\ yr^{-1}$)	Percent (%)	Amount ($t\ km^{-2}\ yr^{-1}$)	Percent (%)
Loess Plateau	1901-1924	4367.6							
	1925-1981	6317.9	4665.2	1950.2	44.7	297.6	15.3	1652.7	84.7
	1982-2016	3475.9	4496.4	-891.8	-20.4	128.8	-14.4	-1020.6	114.4
Hilly and gully plateau	1901-1931	7758.0							
	1932-1981	10770.0	9152.9	3012.0	38.8	1394.9	46.3	1617.1	53.7
	1982-2016	6146.5	8543.7	-1611.5	-20.8	785.7	-48.8	-2397.2	148.8
High-plain plateau	1901-1924	4811.8							
	1925-1981	7301.4	4828.1	2489.6	51.7	16.3	0.7%	2473.4	99.3
	1982-2016	3972.2	4647.7	-839.7	-17.4	-164.1	19.5	-675.6	80.5
Rocky mountainous area	1901-1931	5745.6							
	1932-1981	8068.3	6821.8	2322.6	40.4	1076.1	46.3	1246.5	53.7
	1982-2016	3360.2	6433.1	-2385.4	-41.5	687.5	-28.8	-3072.9	128.8
Fen-Wei river valley	1901-1931	2925.2							
	1932-1981	4246.3	3372.5	1321.1	45.2	447.2	33.9	873.8	66.1
	1982-2016	2036.7	3216.1	-888.5	-30.4	290.9	-32.7	-1179.4	132.7
Hetao alluvial plains	1901-1924	857.8							
	1925-1981	1330.2	874.3	472.5	55.1	16.6	3.5	455.9	96.5
	1982-2016	781.4	833.4	-76.4	-8.9	-24.3	31.8	-52.0	68.2
Deserts	1901-1931	661.2							
	1932-1981	964.2	727.1	303.0	45.8	65.8	21.7	237.2	78.3
	1982-2016	652.0	689.5	-9.2	-1.4	28.3	-306.0	-37.5	406.0

a refers to the total changes in erosion rates from the comparison period to the reference period, while b and c refer to the contribution of precipitation change and human activity to the total change. For the Loess Plateau, high-plain plateau and Hetao alluvial plains, the reference period is 1901-1924 and the comparison periods are 1925-1981 and 1982-2016. For hilly and gully plateau, rocky mountainous area, Fen-Wei river valley, and deserts, the reference period is 1901-1931 and the comparison periods are 1932-1981 and 1982-2016.

4 Discussion

4.1 Spatiotemporal changes of erosion rates

Long-term historic (e.g. century scale) erosion rate assessments have either been rarely undertaken (Rodway-Dyer et al., 2010；Garcia-Ruiz et al., 2015; Gonzalez et al., 2016; Li et al., 2020b) or subject to spatial heterogeneity due to the difference in measurement methods or scale of measurements (Kirkby et al., 1996; Garcia-Ruiz et al., 2015; Borrelli et al., 2017). Based on century-scale process modelling, we reconstructed historic erosion rates for the entire Loess Plateau for the first time, and validated the results using field measurements. The satisfactory modelling accuracy demonstrated that the method employed in our study worked well. This has important implications for historic erosion rate assessment in other parts of the world. For example, our method can be used to derive erosion rates across large areas with scarce erosion rate assessments, such as the Tibetan Plateau (Teng et al., 2018) and remote peatlands (Li et al., 2018). The reconstructed erosion rates can then be used for further analysis with erosion drivers, providing a direct reference for erosion conservation.

Based on the reconstructed erosion rates for the Loess Plateau, we found that decadal average erosion rates and the area with intensive erosion (Sun et al., 2014) increased between the 1930s and 1970s, decreased between the 1980s and 2000s to a historic low level (since 1901) and rebounded after 2010. This temporal change pattern is roughly consistent with the fluctuations of sediment load of the Yellow River, which was relatively low before the 1930s, increased until the -1960s and decreased since the 1980s (He et al., 2004; 2006). However, sediment yield at catchment outlets can no longer represent the detailed distribution of soil erosion, particularly when eroded particles are trapped by check-dams and reservoirs established in gullies and river channels in the region (Li et al., 2020b). Compared to previous erosion rate assessments focusing on the 1980s onwards (e.g. Li et al., 2019; Sun et al., 2014), our study is able to reach broader conclusions. This is because previous modelling results may be subject to bias given that soil erosion rates and the area of very intensive erosion (> 8000 t km^{-2} yr^{-1}) since the 1980s have sharply decreased compared to previous decades. In terms of century-scale modelling, we found that the spatial distribution of very intensive erosion shifted mainly within the hilly-gully plateau and high-plain plateau, and sometimes extended to the rocky mountainous area (1930s-1970s) (Figure 1). The central Loess Plateau was particularly subject to severe erosion even during the period with historic low erosion rates (e.g. 2000s).

4.2 Impacts of human activities and extreme weather events

We demonstrated that human activities played a dominant role and climate change played a secondary role in historic erosion changes on the Loess Plateau during 1901-2016. This is consistent with previous studies investigating the contribution of climate change and human activities on soil erosion / sediment flux on the Plateau (e.g. Li et al., 2019; Guo et al., 2019; Zheng et al., 2019; Xu et al., 2021). However, most previous studies found that human activities and climate change contributed to the reduction of erosion / sediment flux rather than the increase of erosion / sediment flux. We found that human-dominated erosion increased during 1925/1932-1981 and decreased during 1982-2016 for the Loess Plateau and its subregions, while precipitation changes intensified erosion on the Loess Plateau and most of its subregions throughout the study period (except High-plain plateau and Hetao alluvial plains). The above discrepancy could be attributed to the difference in study periods (and thus different reference periods), given that different attribution analysis methods employed in previous studies have been demonstrated to produce comparable results for the same environmental settings (Zhao et al., 2018). Previous studies on erosion rate assessment were mainly conducted for the 1980s onwards, while those on sediment flux investigation primarily focused on the 1920s onwards. In earlier studies the contribution of climate change and human activities was assessed using a reference period with higher erosion rates than that used in our study (e.g. 1901-1924/1901-1930). Therefore, our study offers new insights into the role that human activities and climate change played in altering loess plateau erosion rates. .

Changes in modelled erosion rates for the Loess Plateau were in accordance with some important social changes. In the 1930s and 1940s, the central Loess Plateau became densely populated because of migration during the anti-invasion war and inner war in China (He et al., 2006). For example, the population of northern Shaanxi province increased from 1.31 million in 1941 to 1.42 million in 1945 (Liu et al., 2012). Given that the awareness of the general public about soil conservation was low, the population increase led to mass devastation of forest and grassland vegetation and thus rapid erosion increase (Figure 1). The end of wars in 1949 and subsequent economic development facilitated a rapid population growth during the 1950s to 1970s. However, China, and particularly on the Loess Plateau, still suffered from low agricultural productivity and firewood shortages. Between 1958 and 1960, China undertook the ‘Great Leap Forward’ policy, and implemented the ‘food for the program’ in agricultural production, largely encouraging cultivation and deforestation (Rozelle et al., 1997). Cropland expansion, particularly on hillslopes, and firewood requirements further reduced forest and grassland vegetation and intensified erosion. Although conservation measures were implemented to control erosion, they did not work well

(Zhao et al., 2013). Overall, because there was a great increase in human interventions without efficient land management or erosion control measures, soil erosion was exacerbated, leading to the expansion of serious erosion between the 1930s and 1970s.

Since the 1980s, China undertook social and economic reforms to control soil erosion and to guarantee food security for inhabitants. The policy “comprehensive management of small watersheds” was launched to integrate the management of hills, water, forests, and croplands, with the aim of reducing sediment and flooding, and improving agricultural production (Wu et al., 2020). The ‘Grain-for-Green’ project, which is the largest ecological restoration program in developing countries and mainly concentrated in the hilly and gully plateau and high-plain plateau, has been implemented since 1999 (Feng et al., 2016). In addition, rapid economic development and urbanization led to a large-scale migration of population from rural areas to cities (Wei et al., 2019), directly reducing the human-land conflict. These factors led to a rapid erosion decrease since the 1980s and particularly low erosion rates during the 2000s. Overall, the decrease of erosion rates since the 1980s to a historic low level directly demonstrates the long-term success of the soil and water conservation measures (Wang et al., 2021). This success is also meaningful for other places in the world suffering from soil erosion, as erosion is also likely to be controlled by intensive conservation measures given that it could be controlled in the harsh Loess Plateau environment.

Although human activities were found to dominate the erosion rate change on the Loess Plateau, we found a rebound of average erosion rates during 2010-2016 on the Plateau that was mainly driven by intensive storms occurring in the hilly and gully plateau in July 2013 (Li et al., 2020a)

(Figure 5). This supported our hypothesis that erosion rate changes may be dominated by different factors over different periods. There have been studies assessing the impacts of extreme rainfall events on soil erosion/sediment flux on the Loess Plateau (e.g. Hu et al., 2019; Wang et al., 2020; Zhao et al., 2021) and other places in the world (e.g. Lana-Renault et al., 2009; Estrany et al., 2009; Wu et al., 2021; Li et al., 2021a). However, they were undertaken mainly at plot / catchment scales and thus they were not able to investigate the impact of intensive events at larger scales (e.g. the whole of the Loess Plateau). We demonstrated that individual storm events had wider implications and may lead to an exceptional increase of mean soil erosion rates over a large region (e.g. the hilly-gully plateau and even the entire Loess Plateau).

On the Loess Plateau, vegetation consumption of water during drier conditions (Jia et al., 2017) is now close to the level beyond which the population will suffer water shortages (Feng et al., 2016; Wang et al., 2018). This creates a scientific challenge because if further revegetation is encouraged to reduce erosion it may lead to water scarcity for the human population. However, without good vegetation cover, extreme rainfall events, which may occur more frequently in the future (Wang et al., 2015), may further increase mean decadal erosion rates. There is also a challenge of maintenance of some conservation measures to withstand future storm events. For example, there was widespread destruction of terraces and roads during storms on 26 July 2017 (Yang et al., 2019; Zhang et al. 2019), further exacerbating soil loss. Therefore, an enhanced erosion control strategy is needed for the Loess Plateau to cope with extreme events in the future.

4.3 Uncertainties and limitations

Our modelling is subject to uncertainties. The major source of uncertainty comes from model input data. A representative and widely applied historical land-use product, HYDE 3.2.1 (Zhang et al., 2021), was used for the derivation of the *C* and *P* factors, given that more accurate historical land-use data were unavailable for the Loess Plateau. In order to overcome the drawbacks of the coarse resolution (~ 8 km), we have resampled the HYDE 3.2.1 dataset to a 1-km resolution during the derivation of *C* and *P* factors, and further incorporated the 300-m CCI_LC dataset for *P* factor derivation. Although resampling did not improve the accuracy of the HYDE 3.2.1 dataset, a smaller grid cell size did facilitate the matching of landuse type with other datasets with higher resolution (e.g. NDVI data). Since data on vegetation cover before 1980 were not available, we reconstructed the NDVI based on the close relationship between precipitation and vegetation on the Loess Plateau (Kong et al., 2018). We acknowledged that the vegetation coverage is impacted by multiple driving factors such as climate conditions and human activities (e.g. agricultural production and revegetation). Thus, our reconstructed NDVI was subject to uncertainties which propagated into modelled erosion rates. However, it was difficult to reconstruct the vegetation coverage with more sophisticated methods (models) given that there were insufficient data (particularly human activity data) to feed them.

RUSLE is an empirical model. The model does not consider the specific erosion processes, possibly limiting its capacity to reflect the response of erosion rates to influencing factors. However, RUSLE enabled long-term and large-scale modelling which was advantageous over contemporary process-based models that are primarily event-based, catchment-scale models, which are not able to model long-term erosion rates over large areas (Li et al., 2017c). Therefore, the use of RUSLE in our study was a compromise. In the future, more effort should be made to develop long-term and large-scale process-based models for the Loess Plateau so that more specific erosion processes can be incorporated.

4.4 Implications for management

Our results have implications for land management. The spatial pattern of modelled erosion rates provides a direct reference for decision makers to identify the key erosion regions within the Loess Plateau. This helps the government to put limited resources towards the most critical locations. For example, we found that the central Loess Plateau was always subject to severe erosion even when the mean erosion rates of the entire Loess Plateau reached an historic low level in the 2000s (Figure 1). This implies that the central Loess Plateau should be the key region for future soil and water conservation.

We found that human activities were dominant drivers of erosion rate changes before the 2000s, while extreme rainfall events accounted for the erosion rate rebound between 2000 and 2016. This suggests that the existing erosion control measures on the Loess Plateau may not be able to cope with extreme rainstorms and erosion rates may increase again if the extreme weather occurs more frequently in the future. Therefore, an enhanced erosion control strategy is needed for the Loess Plateau, and particularly for the central Loess Plateau, which is the area most sensitive to erosion. However, given the contradiction between the water resource scarcity and soil conservation discussed above, enhanced erosion control may need to be achieved through supporting revegetation that consumes less soil moisture (e.g. using species that are more drought tolerant) (Wang et al., 2016) and improved engineering measures (e.g. stormwater capture) (Zhang et al., 2014).

Our results also have global implications for environmental protection. Global warming is expected to intensify both drought and flash floods, which are serious threats to fragile terrestrial environments (Borrelli et al., 2020; Ornes, 2018; Tabari, 2020; Yin et al., 2018). Increasing risks of drought and floods directly challenges the resilience of existing measures and demands innovative new nature-based geoengineering methods for environmental protection.

5 Conclusions

We assessed the spatiotemporal pattern of erosion rates over the entire Chinese Loess Plateau between 1901 and 2016 using the RUSLE model and attributed the erosion rate changes to human activities and climatic drivers. The RUSLE modelling results were validated with sediment yield measurements from 22 catchments between 1919 and 1969, during which time sediment yields were very representative of erosion rates within catchments, as check dams and barriers were not widespread during this period. Modelling results showed that decadal average soil erosion rates and the total area with intensive erosion (> 5,000 t km^{-2} yr^{-1}) experienced a sharp increase from the 1930s to 1970s, followed by a decline to an historic low during the 2000s. Mean erosion rates for the Loess Plateau in the 2000s decreased by 54.3 % compared to the 1970s. However, a recent increase in erosion rates was observed between 2010 and 2016. Human activities were the dominant direct drivers of the historical rise and fall of erosion rates until 2010. Extensive deforestation and farming driven by population increase were responsible for the intensifying erosion between the 1930s and 1970s while policy-driven conservation schemes and revegetation led to the reduction thereafter. However, the recent increase in erosion rates between 2010 and 2016 was found to be mainly driven by extreme rainstorms. This demonstrates a new challenge for ecological recovery as extreme climate events are likely to be exacerbated further by global warming. Compounded with human water shortages, ecological recovery of the Loess Plateau demands a strengthened innovative erosion control strategy.

Acknowledgements

This work was financially supported by National Natural Science Foundation of China (41807063, 41977059) and the Special Funds of the National Natural Science Foundation of China (42041004).

Data availability

The raw data for the derivation of RUSLE inputs can be obtained through the corresponding links and references in the section 2.2.1 'RUSLE description and implementation'. RUSLE inputs and outputs have been provided in the text, figures, tables and supporting information. Other data can be obtained from corresponding authors upon reasonable request.

Author contributions

Xingmin Mu, Guangju Zhao and Pengfei Li conceived the idea and designed the research. Pengfei Li, Jiannan Chen and Guangju Zhao analyzed data, produced figures and tables, and drafted the manuscript. Bintao Liu implemented RUSLE. Pengfei Li, Joseph Holden, Peili Wu, Guangju Zhao, Bintao Liu, Jinfei Hu, Faith Ka Shun Chan and Xingmin Mu refined the manuscript and provided additional interpretation of the findings.

Conflict of Interests

The authors declare no conflict of interests.

References

Armstrong, A. (2014). Yellow River erosion. *Nature Geoscience, 249*, 7. https://doi.org/10.1038/ngeo2135

Batista, P. V., Davies, J., Silva, M. L., and Quinton, J. N. (2019). On the evaluation of soil erosion models: Are we doing enough ? *Earth-Science Reviews, 197*, 102898. https://doi.org/10.1016/j.earscirev.2019.102898

Best, J. (2019). Anthropogenic stresses on the world's big rivers. *Nature Geoscience, 12*, 7-21. https://doi.org/10.1038/s41561-018-0262-x

Bontemps, S., Boettcher, M., Brockmann, C., Kirches, G., Lamarche, C., Radous, J.,et al. (2015). *Multi-year global land cover mapping at 300 m and characterization for climate modelling: Achievements of the land cover component of the ESA climate change initiative.* Paper presented at the the 36th International Sysposium on Remote Sensing of Environment, Berlin, Germany.

Borelli, P., Robinson, D. A., Fleischer, L. R., Lugato, E., Ballabio, C., Alewell, C., et al. (2017). An assessment of the global impact of 21st century land use change on soil erosion. *Nature Communications, 8*(1), 2013. https://doi.org/doi: 10.1038/s41467-017-02142-7

Borrelli, P., Robinson, D. A., Panagos, P., Lugato, E., Yang, J. E., Alewell, C., et al. (2020). Land use and climate change impacts on global soil erosion by water (2015-2070). *Proceedings of the National Academy of Sciences of the United States of America, 117*(36), 21994-22001. https://doi.org/10.1073/pnas.2001403117

Cai, Q. (2001). Soil erosion and management on the Loess Plateau. *Journal of Geographical Sciences, 11*(1), 53-70. https://doi.org/ 10.1007/bf02837376

Cluis, D. A. (1983). Visual techniques for the detection of water quality trends: double-mass curves and CUSUM functions. *Environmental Monitoring and Assessment, 3*(2), 173-184. https://doi.org/10.1007/BF00398846

Estrany, J., Garcia, C., and Batalla, R. J. (2009). Suspended sediment transport in a small Mediterranean agricultural catchment. *Earth Surface Processes and Landforms,* 34(7), 929-940. https://doi.org/10.1002/esp.1777

Evans, M. and Warburton J. (2005). Sediment budget for an eroding peat-moorland catchment in northern England. *Earth Surface Processes and Landforms,* 30(5), 557-577. https://doi.org/10.1002/esp.1153

Evans, M., Warburton J., and Yang J. (2006). Eroding blanket peat catchments: Global and local implications of upland organic sediment budgets. *Geomorphology*, 79(1-2), 45-57. https://doi.org/10.1016/j.geomorph.2005.09.015

Feng, X., Fu, B., Piao, S., Wang, S., Ciais, P., Zeng, Z., et al. (2016). Revegetation in China's Loess Plateau is approaching sustainable water resource limits. *Nature Climate Change*. https://doi.org/10.1038/nclimate3092

Garcia-Ruiz, J. M., Begueria S., Nadal-Romero E., Gonzalez-Hidalgo J. C., Lana-Renault N., and Sanjuan Y. (2015). A meta-analysis of soil erosion rates across the world. Geomorphology 239, 160-173. https://doi.org/10.1016/j.geomorph.2015.03.008

Guan, Y., S. Yang, C. Zhao, H. Lou, K. Chen, C. Zhang and B. Wu (2021). Monitoring long-term gully erosion and topographic thresholds in the marginal zone of the Chinese Loess Plateau. *Soil & Tillage Research, 205*, 104800. https://doi.org/10.1016/j.still.2020.104800

Guo, Q., Ding Z., Qin W., Gao W., Lu W., Xu X., and Yin Z. (2019). Changes in sediment load in a typical watershed in the tableland and gully region of the Loess Plateau, China. *Catena,* 182, 104132. https://doi.org/10.1016/j.catena.2019.104132

Gonzalez, V. S., Bierman P. R., Nichols K. K., and Rood D. H. (2016). Long-term erosion rates of Panamanian drainag basins determined using in situ Be-10. Geomorphology 275, 1-15. https://doi.org/10.1016/j.geomorph.2016.04.025

He, X., Tang, K., and Zhang, X. (2004). Soil erosion dynamics on the Chinese Loess Plateau in the last 10,000 years. *Mountain Research and Development, 24*(4), 342-347. https://doi.org/10.2307/3674513

He, X., Zhou, J., Zhang, X., and Tang, K. (2006). Soil erosion response to climatic change and human activity. *Regional Environmental Change*(6), 62-70. https://doi.org/10.1007/s10113-005-0004-7

Hu, J., Gao, P., Mu, X., Zhao, G., Sun, W., Li P., and Zhang L. (2019). Runoff-sediment dynamics under different flood patterns in a Loess Plateau catchment, China. *Catena*, 173, 234-245. https://doi.org/10.1016/j.catena.2018.10.023

Jiao, Q., Li, R., Wang, F., Mu, X., Li P., and An C. (2016). Impacts of re-vegetation on surface soil moisture over the Chinese Loess Plateau based on remote sensing datasets. *Remote Sensing, 8*(2): 156. https://doi.org/10.3390/rs8020156

Jia, X., Shao, M. a., Zhu, Y., and Luo, Y. (2017). Soil moisture decline due to afforestation across the Loess Plateau, China. *Journal of Hydrology, 546*, 113-122. https://doi.org/10.1016/j.jhydrol.2017.01.011

Jiang, Z., Zheng, F., and Wu, M. (2005). Prediction model of water erosion on hillslopes. *Journal of Sediment Research*(4), 1-6. https://doi.org/10.16239/j.cnki.0468-155x.2005.04.001. (in

Chinese with English abstract).

Karger, D.N., and Zimmermann, N.E. (2018). CHELSAcruts - High resolution temperature and precipitation timeseries for the 20th century and beyond. *EnviDat*. http://dx.doi.org/10.16904/envidat.159

Klein Goldewijk, K., Beusen, A., Doelman, J., and Stehfest, E. (2017). Anthropogenic land use estimates for the Holocene - HYDE 3.2. *Earth System Science Data, 9*(2), 927-953. https://doi.org/10.5194/essd-9-927-2017

Kong, D., Miao C., Duan Q., Lei X., and Li H. (2018). Vegetation-climate interactions on the Loess Plateau: A nonlinear granger causality analysis. *Journal of Geophysical Research: Atmospheres*, 123(19), 11068-11079. https://doi.org/10.1029/2018JD029036

Lana-Renault, N., and Regues, D. (2009). Seasonal patterns of suspended sediment transport in an abandoned farmland catchment in the central Spanish Pyrenees. *Earth Surface Processes and Landforms*, 34(9), 1291-1301. https://doi.org/10.1002/esp.1825

Li, C., Grayson R., Holden J., and Li P. (2018). Erosion in peatlands: Recent research progress and future directions. *Earth-Science Reviews*, 185, 870-886. https://doi.org/10.1016/j.earscirev.2018.08.005

Li, D., Lu, X., Overeem, I., Walling, D. E., Syvitski, J., Kettner, A. J., Bookhagen, B., Zhou, Y., and Zhang T. (2021a). Exceptional increases in fluvial sediment fluxes in a warmer and wetter high mountain Asia. *Science* 374 (6567), 599-603. https://doi.org/10.1126/science.abi9649

Li, J., Liu, Q., Feng, X., Shi, W., Fu, B., Lv, Y., and Liu, Y. (2019). The synergistic effects of afforestation and the construction of check-dams on sediment trapping: Four decades of evolution on the Loess Plateau, China. *Land Degradation & Development, 30*(6), 622-635.

https://doi.org/ 10.1002/ldr.3248

Li, J., Peng, S., and Li, Z. (2017a). Detecting and attributing vegetation changes on China's Loess Plateau. *Agricultural and Forest Meteorology, 247*(260-270). https://doi.org/10.1016/j.agrformet.2017.08.005

Li, M., Ma, C., Du, C., Yang, W., Lyu, L., and Wang, X. (2020a). Landslide response to vegetation by example of July 25–26, 2013, extreme rainstorm, Tianshui, Gansu Province, China. *Bulletin of Engineering Geology and the Environment,* 80(2) ,1-14. https://doi.org/10.1007/S10064-020-02000-9

Li, P., Holden, J., Irvine, B., and Mu, X. (2017b). Erosion of Northern Hemisphere blanket peatlands under 21st-century climate change. *Geophysical Research Letters*, 44(8), 3615-3623. https://doi.org/10.1002/2017GL072590

Li, P., Hao, M., Hu, J., Gao, C., Zhao, G., Chan, F. K. S., et al. (2021b). Spatiotemporal patterns of hillslope erosion investigated based on field scouring experiments and terrestrial laser scanning. *Remote Sensing, 13*(9): 1674. https://doi.org/10.3390/rs13091674

Li, P., Mu, X., Holden, J., Wu, Y., Irvine, B., Wang, F., et al. (2017c). Comparison of soil erosion models used to study the Chinese Loess Plateau. *Earth-Science Reviews, 170*, 17-30. https://doi.org/10.1016/j.earscirev.2017.05.005

Li, P., Zang, Y., Ma, D., Yao, W., Holden, J., Irvine, B., and Zhao, G. (2020b). Soil erosion rates assessed by RUSLE and PESERA for a Chinese Loess Plateau catchment under land-cover changes. *Earth Surface Processes and Landforms, 45*(3), 707-722. https://doi.org/10.1002/esp.4767

Li, Y., Zhang, X., Cao, Z., Liu, Z., Lu, Z., and Liu, Y. (2021c). Towards the progress of ecological restoration and economic development in China's Loess Plateau and strategy for more sustainable development. *Science of the Total Environment, 756*, 143676. https://doi.org/ 10.1016/j.scitotenv.2020.143676

Liu, B., Nearing, M., and Risse, L. (1994). Slope gradient effects on soil loss for steep slopes. *Transactions of the ASAE, 37*(6), 1835-1840. https://doi.org/ 10.13031/2013.28273

Liu, B., Xie, Y., Li, Z., Liang, Y., Zhang, W., Fu, S., et al.(2020). The assessment of soil loss by water erosion in China. *International Soil and Water Conservation Research, 8*(4), 430-439. https://doi.org/10.1016/j.iswcr.2020.07.002

Liu, G., Hu, F., Abd Elbasit, M. A., Zheng, F., Liu, P., Xiao, H., et al. (2018). Holocene erosion trigerred by climate change in the central Loess Plateau of China. *Catena, 160*, 103-111. https://doi.org/10.1016/j.catena.2017.09.013

Liu, Y., Xu, Y., and Liu, Y. (2012). Population growth and temporal-spatial differentiation in Loess Plateau region in the last 2000 years. *Progress in Geography, 31*(2), 156-166. https://doi.org/10.11820/dlkxjz.2012.02.004 (in Chinese with English abstract).

McCool, D., Foster, G., Mutchler, C., and Meyer, L. (1989). Revised slope length factor for the Universal Soil Loss Equation. *Transactions of the American Society of Agricultural and Engineers (ASAE), 32*(5), 1571-1576. https://doi.org/ 10.13031/2013.31192

McCool, D., Foster, G., and Weesies, G. (1997). *Predicting Soil Erosion by Water: A Guide to Conservation Planning with the Revised Universal Soil Loss Equation (RUSLE)*: USDA.

Milliman, J. and Farnsworth K. (2011). River discharge to the coastal ocean - A global synthesis. Cambridge, Cambridge University Press.

Milodowski, D. T., Hancock, S., Silvestri, S., and Mudd, S. M. (2020). Linking life and landscape with remote sensing. In P. Tarolli and S. M. Mudd (Eds.), *Remote Sensing of Geomorphology* (Vol. 23, pp. 129-182): Elsevier. https://doi.org/10.1016/B978-0-444-

64177-9.00005-9

Montgomery, D. R. (2007). Soil erosion and agricultural sustainability. *Proceedings of the National Academy of Sciences of the United States of America, 104*(33), 13268-13272. https://doi.org/10.1073/pnas.0611508104

Mu, X., Zhang, X., Shao, H., Gao, P., Wang, F., Jiao, J., and Zhu, J. (2012). Dynamic changes of sediment discharge and the influencing factors in the Yellow River, China, for the recent 90 years. *Clean-Soil, Air, Water, 40*(3), 303-309. https://doi.org/10.1002/clen.201000319

Mu, X., Zhao, G., Gao, P., and Sun, W. (2019). *New patterns of the changes in runoff and sediment yield on the Chinese Loess Plateau*. Beijing: Science Press (in Chinese).

Ornes, S. (2018). Core Concept: How does climate change influence extreme weather? Impact attribution research seeks answers. *Proceedings of the National Academy of Sciences, 115*(33), 8232-8235. https://doi.org/10.1073/pnas.1811393115

Ren, M., and Zhu, X. (1994). Anthropogenic influences on changes in the sediment load of the Yellow River, China, during the Holocene. *The Holocene, 4*(3), 314-320. https://doi.org/10.1177/095968369400400311

Renard, K., Foster, G., Weesies, G., and Porter, J. (1991). RUSLE: Revised universal soil loss equation. *Journal of Soil and Water Conservation, 46*(1), 30-33. https://doi.org/10.1002/9781444328455.ch8

Rodrigo-Comino, J. (2018). Five decades of soil erosion research in "terroir". The State-of-the-Art. *Earth-Science Reviews, 179*, 436-447. https://doi.org/10.1016/j.earscirev.2018.02.014

Rodway-Dyer, S. J., and Walling D. E. (2010). The use of 137Cs to establish longer-term soil erosion rates on footpaths in the UK. *Journal of Environmental Management* 91(10), 1952-1962. https://doi.org/10.1016/j.jenvman.2010.04.014

Rozelle, S., Huang, J., and Zhang, L. (1997). Poverty, population and environmental degradation in China. *Food Policy, 22*(3), 229-251.

Searcy, J. K., and Hardison, C. H. (1960). Double-mass curves. *Bytes*. http://udspace.udel.edu/handle/19716/1592

Shmilovitz, Y., Marra, F., Wei, H., Argaman, E., Nearing, M., Goodrich, D., Assouline S., and Morin, E. (2021). Frequency analysis of storm-scale soil erosion and characterization of extreme erosion events by linking the DWEPP model and a stochastic rainfall generator. *Science of the Total Environment*, 787, 147609. https://doi.org/10.1016/j.scitotenv.2021.147609

Sun, P., Wu, Y., Wei, X., Sivakumar, B., Qiu, L., Mu, X., et al. (2020). Quantifying the contributions of climate variation, land use change, and engineering measures for dramatic reduction in streamflow and sediment in a typical loess watershed, China. *Ecological Engineering, 142*, 105611. https://doi.org/10.1016/j.ecoleng.2019.105611

Sun, W., Shao, Q., Liu, J., and Zhai, J. (2014). Assessing the effects of land use and topography on soil erosion on the Loess Plateau in China. *Catena, 121*, 151-163. https://doi.org/10.1016/j.catena.2014.05.009Tabari, H. (2020). Extreme value analysis dilemma for climate change impact assessment on global flood and extreme precipitation. *Journal of Hydrology, 593*, 125932. https://doi.org/10.1016/j.jhydrol.2020.125932

Teng, H., Liang Z., Chen S., Liu Y., Visarra Rossel R. A., Chappell A., Yu W., and Shi Z. (2018). Current and future assessments of soil erosion by water on the Tibetan Plateau based on RUSLE and CMIP5 climate models. *Science of the Total Environment,* 635, 673-686. https://doi.org/10.1016/j.scitotenv.2018.04.146

Tong, Y., Zhang, W., Wang, X., Couture, R.-M., Larssen, T., Zhao, Y., et al. (2017). Decline in

Chinese lake phosphorus concentration accompanied by shift in sources since 2006. *Nature Geoscience, 10*(7), 507-511. https://doi.org/10.1038/ngeo2967

Tsunekawa, A., G. Liu, N. Yamanaka and S. Du (2014). *Restoration and Development of the Degraded Loess Plateau, China*. Springer, Tokyo.

Wang, N., Jiao J., Bai L., Zhang Y., Chen Y., Tang B., Liang Y., Zhao C., and Wang H. (2020). Magnitude of soil erosion in small catchments with different land use patterns under an extreme rainstorm event over the Northern Loess Plateau, China. *Catena*, 195, 104780. https://doi.org/10.1016/j.catena.2020.104780

Wang, H., and Sun, F. (2021). Variability of annual sediment load and runoff in the Yellow River for the last 100 years (1919-2018). *Science of the Total Environment, 758*, 143715. https://doi.org/10.1016/j.scitotenv.2020.143715

Wang, S., Fu, B., Chen, H., and Liu, Y. (2018). Regional development boundary of China's Loess Plateau: Water limit and land shortage. *Land Use Policy, 74*, 130-136. https://doi.org/10.1016/j.landusepol.2017.03.003

Wang, S., Fu, B., and Liang, W. (2016). Developing policy for the Yellow River sediment sustainable control. *National Science Review, 3*(2), 162-164. https://doi.org/10.1093/nsr/nww031

Wang, S., Fu, B., Piao, S., Lü, Y., Ciais, P., Feng, X., and Wang, Y. (2015). Reduced sediment transport in the Yellow River due to anthropogenic changes. *Nature Geoscience, 9*(1), 38-41. https://doi.org/10.1038/ngeo2602

Wang, X., Wang, Z., Xiao, J., He, M., Zhang, F., Pan, Y., et al. (2021). Soil erosion fluxes on the central Chinese Loess Plateau during CE 1811 to 1996 and the roles of monsoon storms and human activities. *Catena, 200*, 105148. https://doi.org/ 10.1016/j.catena.2021.105148

Wei, J., Zheng, K., Zhang, F., Fang, C., Zhou, Y., Li, X., et al. (2019). Migration of rural residents to urban areas drives grassland vegetation increase in China's Loess Plateau. *Sustainability, 11*(23), 6764. https://doi.org/10.3390/su11236764

Wen, X., and Deng, X. (2020). Current soil erosion assessment in the Loess Plateau of China: A mini-review. *Journal of Cleaner Production, 276*, 123091. https://doi.org/10.1016/j.jclepro.2020.123091

Wu, J., J. Baartman, E. M., and Pedro Nunes, J. (2021). Testing the impacts of wildfire on hydrological and sediment response using the OpenLISEM model. Part 2: Analyzing the effects of storm return period and extreme events. *Catena,* 207, 105620. https://doi.org/10.1016/j.catena.2021.105620

Wu, X., Wei, Y., Fu, B., Wang, S., Zhao, Y., and Moran, E. (2020). Evolution and effects of the social-ecological system over a millennium in China's Loess Plateau. *Science Adcances, 6*(41), eabc0276. https://doi.org/10.1126/sciadv.abc0276

Xin, Z., Xu, J., and Zheng, W. (2008). Spatiotemporal variations of vegetation cover on the Chinese Loess Plateau (1981-2016): Impacts of climate changes and human activities. *Science in China Series D: Earth Sciences, 50*(1), 67-78. https://doi.org/10.1007/s11430-007-0137-2

Xu, J., Jiang X., Sun H., Xu H., Zhong X., Liu B., and Li L. (2021). Driving forces of nature and human activities on water and sediment changes in the middle reaches of the Yellow River in the past 100 years. *Journal of Soils and Sediments,* 21, 2450-2464. https://doi.org/10.1007/s11368-021-02952-9

Yang, B., Wang, W., Guo, M., Guo, W., Wang, W., Kang, H., et al. (2019). Soil erosion of unpaved loess roads subjected to an extreme rainstorm event: a case study of the Jiuyuangou watershed on the Loess Plateau, China. *Journal of Mountain Science, 16*, 1396-1407. https://doi.org/10.1007/s11629-018-5211-z

Yang, X., W. Sun, P. Li, X. Mu, P. Gao and G. Zhao (2018). "Reduced sediment transport in the Chinese Loess Plateau due to climate change and human activities." *Science of the Total Environment,642*: 591-600. https://doi.org/10.1016/j.scitotenv.2018.06.061

Yin, J., Gentine, P., Sha, Z., Sullivan, S. C., and Guo, S. (2018). Large increase in global storm runoff extremes driven by climate and anthropogenic changes. *Nature Communications, 9*(1), 4389. https://doi.org/10.1038/s41467-018-06765-2

Zhang, D., Fand, X., and Yand, L. E. (2021). Comparison of the HYDE cropland data over the past millennium with regional historical evidence from Germany. *Regional Environmental Change*, 21(1), 15. https://doi.org/10.1007/s10113-020-01735-1

Zhang, F., Xing, Z., Rees, H. W., Dong, Y., Li, S., and Meng, F. (2014). Assessment of effects of two runoff control engineering practices on soil water and plant growth for afforestation in a semi-arid area after 10 years. *Ecological Engineering*, 64, 430-442. https://doi.org/10.1016/j.ecoleng.2013.12.024

Zhang, K., Peng, W., and Yang, H. (2007). Soil erodibility and its estimation for agricultural soil in China. *Acta Pedologica Sinica, 44*(1), 7-13. https://doi.org/10.1016/j.jaridenv.2007.11.018 (in Chinese with English abstract).

Zhang, W., and Fu, J. (2003). Rainfall erosivity estimation under different rainfall amount. *Resources Science, 25*(1), 35-41.https://doi.org/10.3321/j.issn:1007-7588.2003.01.006 (in Chinese with English abstract).

Zhang, Y., Zhao, Y., Liu, B., Wang, Z., and Zhuang, S. (2019). Rill and gully erosion on unpaved roads under heavy rainfall in a agricultural watersheds on China's Loess Plateau.

Agricuture, Ecosystems and Environment, 284, 106580. https://doi.org/10.1016/j.agee.2019.106580

Zhao, G., Mu X., Jiao J., Gao P., Sun W., Li E., Wei Y., and Huang J. (2018). Assessing the response of sediment load variation to climate change and human activities with six different approaches. *Science of the Total Environment,* 639, 773-784. https://doi.org/10.1016/j.scitotenv.2018.05.154

Zhao, G., Mu, X., Wen, Z., Wang, F., and Gao, P. (2013). Soil erosion, conservation, and eco-environment changes in the loess plateau of China. *Land Degradation & Development, 24*(5), 499-510. https://doi.org/10.1002/ldr.2246

Zhao, L., Fang Q., Hou R., and Wu F. (2021). Effect of rainfall intensity and duration on soil erosion on slopes with different microrelief patterns. *Geoderma*, 396, 115085. https://doi.org/10.1016/j.geoderma.2021.115085

Zheng, H., Miao, C., Wu, J., Lei, X., Liao, W., and Li, H. (2019). Temporal and spatial variations in water discharge and sediment load on the Loess Plateau, China: A high-density study. Science of the Total Environment, 666, 875-886. https://doi.org/10.1016/j.scitotenv.2019.02.246